occurred in an extensional rift setting. This setting is not consistent with models for the formation of MVT mineralization in which gravity-driven fluid flow is initiated by compressional tectonism (*15*, *20*). Compaction-driven fluid flow due to rapid sedimentation during subsidence (*21*) may be the mechanism that transported base metals out of the Fitzroy Trough to the Lennard Shelf. This mineralization age is not consistent with the hydrocarbon-driven fluid flow model in which MVT mineralization of the Lennard Shelf was linked to a mid-Carboniferous sea level drop and consequent rapid generation of hydrocarbons within the Fitzroy Trough (*22*).

Radiometric ages for ore-stage minerals in MVT deposits have been obtained only in the last 5 years. In providing a test for the temporal relation between hypothesized cause and effect, these ages, along with recent paleomagnetic ages, have been a major force in driving the evolution of genetic models; for example, from a model in which one orogeny formed all MVT deposits in the United States (*2*), to a model in which MVT deposits formed in various orogenies at different times in Earth's history (with the implication that MVT deposits can only be formed by means of an orogeny) (*3–6*, *14*), to a model that infers they can also form in a rifting environment (*7*, *16*, *23*).

The $^{232}$Th-$^{208}$Pb and $^{238}$U-$^{206}$Pb dating methods may also have considerable value for determining the absolute ages of calcite found in other geologic settings, including other kinds of ore deposits, salt domes, fault zones, speleothems, and petroleum reservoir rocks. The analytical approach is applicable to calcite of any geologic age and so extends calcite geochronology beyond the U-Th disequilibrium method.

## REFERENCES AND NOTES

1. D. A. Sverjensky, *Ann. Rev. Earth Planet. Sci.* **14**, 177 (1986).
2. S. Nakai, A. N. Halliday, S. E. Kesler, H. D. Jones, *Nature* **346**, 354 (1990).
3. J. C. Brannon, F. A. Podosek, R. K. McLimans, *ibid.* **356**, 509 (1992).
4. S. Nakai *et al.*, *Geochim. Cosmochim. Acta* **57**, 417 (1993).
5. J. N. Christensen, A. N. Halliday, S. E. Kesler, D. F. Sangster, *Geol. Soc. Am. Abstr. Prog.* **25**, 471 (1993).
6. J. T. Chesley, A. N. Halliday, T. K. Kyser, P. G. Spry, *Econ. Geol.* **89**, 1192 (1993).
7. J. N. Christensen, A. N. Halliday, J. R. Vearncombe, S. E. Kesler, *ibid.* **90**, 877 (1995).
8. J. C. Brannon, F. A. Podosek, R. K. McLimans, in *Proceedings of the Geology and Geochemistry of MVT Ore Deposits*, Geological Society of America, Rolla, MO, 29 and 30 March 1993, K. Shelton and R. Hagni, Eds. (Univ. of Missouri–Rolla Press, Rolla, MO, 1993), pp. 95–103.
9. P. E. Smith, R. M. Farquhar, R. G. Hancock, *Earth Planet. Sci. Lett.* **105**, 474 (1991).
10. D. F. Sangster, in *Geology and Genesis of Mineral Deposits in Ireland*, C. J. Andrew, R. W. A. Crowe, S. Finlay, W. M. Pennell, J. F. Pyne, Eds. (Irish Association for Economic Geology, Dublin, Ireland, 1986), pp. 625–633.
11. R. D. Hagni and O. R. Grawe, *Econ. Geol.* **59**, 449 (1964); S. R. Blasch and R. M. Coveney Jr., *Geochim. Cosmochim. Acta* **52**, 1007 (1988); D. C. Brockie, E. H. Hare, J. R. Dingess, in *Ore Deposits of the United States 1933–1967*, J. D. Ridge, Ed. (American Institute of Mining, Metallurgical, and Petroleum Engineers, New York, 1968), vol. 1, pp. 400–430; V. M. Ragan, *Econ. Geol.* **89**, 1411 (1994).
12. E. E. Angino, E. D. Goebel, T. C. Waugh, in *Proceedings of the Third International Geochemical Exploration Symposium*, Toronto, Canada, 16 to 18 April 1970, R. W. Boyle and J. I. McGerrigle, Eds. (Canadian Institute of Mining and Metallurgy, Toronto, 1971), pp. 453–456.
13. M. B. Goldhaber *et al.*, *Econ. Geol.*, in press.
14. M. J. Wisniowiecki, R. Van der Voo, C. McCabe, W. C. Kelly, *J. Geophys. Res.* **88**, 6540 (1983); H. Pan, D. T. A. Symons, D. F. Sangster, *Can. J. Earth Sci.* **27**, 923 (1990); D. T. A. Symons and D. F. Sangster, *Econ. Geol.* **86**, 1 (1991); M. T. Lewchuk and D. T. A. Symons, *Geology* **23**, 233 (1995); D. T. A. Symons, *Econ. Geol.* **89**, 438 (1994).
15. D. L. Leach and E. L. Rowan, *Geology* **14**, 931 (1986); J. Oliver, *ibid.*, p. 99; C. M. Bethke and S. A. Marshak, *Ann. Rev. Earth Planet. Sci.* **18**, 287 (1990); J. Oliver, *Earth Sci. Rev.* **32**, 77 (1992); G. Garven, *Ann. Rev. Earth Planet. Sci.* **23**, 89 (1995).
16. A. McManus and M. W. Wallace, *Econ. Geol.* **87**, 189 (1992).
17. L. A. Tompkins, V. A. Pedone, M. T. Roche, D. I. Groves, *ibid* **89**, 450 (1994).
18. J. M. Kennard, M. J. Jackson, K. K. Romine, R. D. Shaw, P. N. Southgate, in *The Sedimentary Basins of Western Australia, Proceedings of the Western Australian Basins Symposium*, Petroleum Exploration Society of Australia, Perth, Western Australia, 14 to 17 August 1994, P. G. Purcell and R. R. Purcell, Eds. (Petroleum Exploration Society of Australia, Perth, Western Australia, 1994), pp. 657–676.
19. J. Begg, *J. Aust. Pet. Explor. Assoc.* **28**, 137 (1987).
20. D. A. Sverjensky and G. Garvin, *Nature* **356**, 481 (1992).
21. L. M. Cathles and A. T. Smith, *Econ. Geol.* **78**, 983 (1983).
22. B. N. Eisenlohr, L. A. Tompkins, L. M. Cathles, M. E. Barley, D. I. Groves, *Geology* **22**, 315 (1994).
23. J. C. Brannon, S. C. Cole, F. A. Podosek, in *Extended Abstracts of the International Field Conference on Carbonate-Hosted Lead-Zinc Deposits*, Society of Economic Geologists, St. Louis, MO, 3 to 6 June 1995 (Society of Economic Geologists, Littleton, CO, 1995), pp. 27–29.
24. K. R. Ludwig, *U.S. Geol. Surv. Open-File Rep. 88-557* (1988).
25. After dissolution, the calcite solutions were spiked with a mixed $^{230}$Th, $^{233}$U, $^{236}$U, $^{205}$Pb tracer solution. Anion exchange chromatography was used to separate U, Th, and Pb from the calcite-spike mix solution. Isotopic analyses for samples from the Jumbo Mine were performed on the Washington University VG 354 thermal emission mass spectrometer with a Daly detector in pulse counting mode; those for samples from Western Australia were performed in single collector mode with a Faraday cup for ion detection.
26. We appreciate the assistance and advice given by M. Tatsumoto, W. Premo, and D. A. Papanastassiou. Supported by NSF grant EAR 93 15048 and University of Missouri-Kansas City Women's Council.

23 August 1995; accepted 30 November 1995

# Redox Stabilization of the Atmosphere and Oceans by Phosphorus-Limited Marine Productivity

Philippe Van Cappellen* and Ellery D. Ingall

Data from modern and ancient marine sediments demonstrate that burial of the limiting nutrient phosphorus is less efficient when bottom waters are low in oxygen. Mass-balance calculations using a coupled model of the biogeochemical cycles of carbon, phosphorus, oxygen, and iron indicate that the redox dependence of phosphorus burial in the oceans provides a powerful forcing mechanism for balancing production and consumption of atmospheric oxygen over geologic time. The oxygen-phosphorus coupling further guards against runaway ocean anoxia. Phosphorus-mediated redox stabilization of the atmosphere and oceans may have been crucial to the radiation of higher life forms during the Phanerozoic.

The fossil and sedimentary records imply that the oxygen level of the atmosphere has remained within a fairly narrow range during most of the Phanerozoic (*1*, *2*). The presence of higher plants and animals on land, for instance, imposes stringent limits on the atmospheric partial pressure of oxygen ($P_{O_2}$) at least since the end of the Devonian. In contrast, early attempts at reconstructing past atmospheric oxygen levels that used simple carbon-plus-sulfur isotope mass-balance models revealed imbalances in the rates of production and consumption of atmospheric oxygen, which should have resulted in unacceptably large fluctuations of $P_{O_2}$ over the course of the Phanerozoic (*3*, *4*). In order to avoid unrealistic excursions of $P_{O_2}$, negative feedbacks have been included in oxygen mass-balance models (*4*, *5*). Mathematically, the feedbacks help reconcile the mass-balance calculations with the geologic evidence, but the true mechanisms that stabilize atmospheric $P_{O_2}$ have been elusive (*6*). Here we show that the marine phosphorus cycle may contain the key oxygen controls, through its involvement in oceanic primary productivity.

The availability of phosphorus limits net primary production of the global ocean on

---

P. Van Cappellen, School of Earth and Atmospheric Sciences, Georgia Institute of Technology, Atlanta, GA 30332-0340, USA.
E. D. Ingall, Marine Science Institute, University of Texas at Austin, Port Aransas, TX 78373-1267, USA.

*To whom correspondence should be addressed.

geologic time scales (7). Consequently, studies have focused on past variations of the input of bioavailable phosphorus to the oceans (8). In addition to the supply rate of nutrient phosphorus from continental weathering, however, marine biological productivity is also a function of how efficiently phosphorus is recycled in the oceans. The recycling of particulate phosphorus deposited on the sea floor depends on the oxygen concentration of the bottom waters: Aerobic conditions enhance the removal of phosphorus by sediments, whereas anaerobic conditions promote the return of dissolved phosphorus to the water column (9). The enhanced retention of phosphorus by sediments underlying oxygenated bottom waters is attributed to active bioaccumulation by aerobic benthic bacteria and phosphate sorption by Fe(III) (hydr)oxides (9).

The redox-sensitive recycling of nutrient phosphorus in the oceans represents a major control on marine net primary production on time scales substantially longer than the oceanic residence time of reactive phosphorus ($\approx$55,000 years). Mass-balance calculations have shown that geologically reasonable fluctuations in ocean ventilation alone could bring about variations in organic carbon burial that are of the same order of magnitude as those inferred from the carbon isotope record (10).

Through its dependence on water column oxygenation, marine phosphorus cycling is also linked to the oxygen content of the atmosphere. In order to analyze this link, we must consider the couplings between phosphorus and all major redox elements: carbon, oxygen, and iron (Fig. 1). We have therefore supplemented our existing model for the phosphorus and carbon cycles (10) with a cycle for iron, in which burial of reactive iron in marine sediments occurs either as oxidized Fe(III) (hydr)oxides or reduced Fe(II) sulfides, and with a simplified oxygen cycle that accounts for the main fluxes affecting the $O_2$ content of the atmosphere. The burial rates of reactive iron were obtained from values in the literature for total iron burial in the ocean and a compilation of chemical extraction data indicating that, on average, 23% of particulate iron in marine sediments is potentially reactive (11). The same data set was used to estimate the relative importance of Fe(III) versus sulfide-bound Fe(II) burial in the modern ocean.

Phosphorus-limited primary production and ocean oxygenation depend on the global-scale vertical circulation of the oceans: Nutrient phosphorus must be brought up to the photic zone and dissolved $O_2$ must be transported downward from the surface ocean. The distribution of iron burial between oxidized and reduced species and the burial efficiencies of organic phosphorus and Fe(III)-bound phosphorus are dependent on the oxygenation of marine bottom waters. Therefore, both the vertical circulation and degree of oxygenation of the oceans are represented in the model, the former through the linear vertical mixing rate, $v_{mix}$ (12), the latter through the degree of anoxicity, DOA (10). Both $v_{mix}$

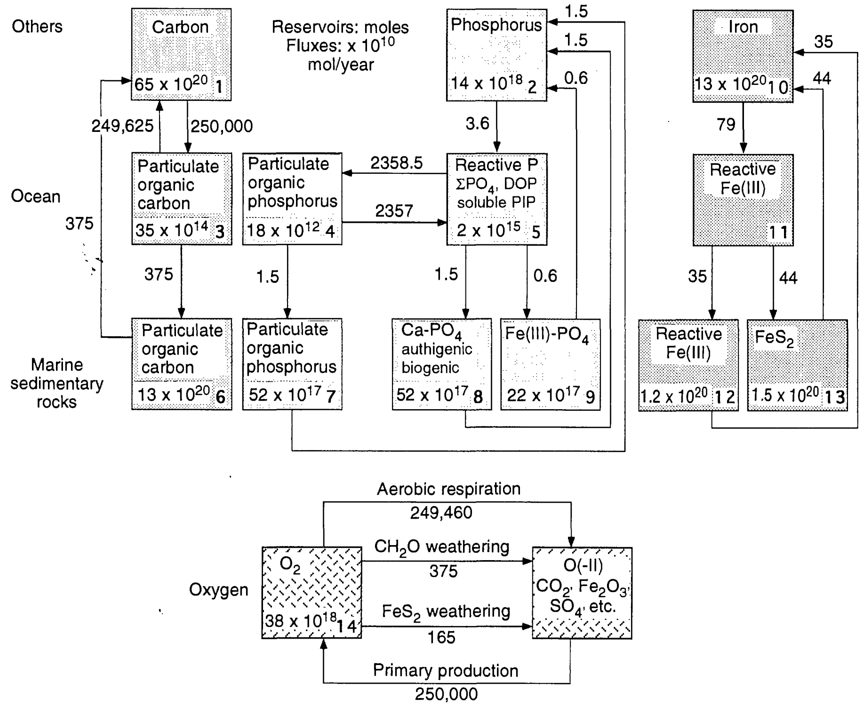

**Fig. 1.** Modern, prehuman steady-state biogeochemical cycles of carbon, phosphorus, iron, and oxygen. The figure identifies the reservoirs (boxes) and material fluxes (arrows) considered in the mass-balance model. Reservoir 1 contains all oxidized carbon in the exogenic cycle, as well as terrestrial organic carbon and marine dissolved organic carbon. Reservoir 2 includes phosphorus stored on land, plus unreactive particulate inorganic phosphorus in the oceans and marine sediments. Terrestrial iron and unreactive marine iron are grouped in reservoir 10. The modern cycles are used to parameterize the flux expressions in Table 1 and they serve as initial conditions in the simulations. The reservoir sizes and fluxes of the carbon and phosphorus cycles were estimated in (10). Reservoirs are measured in moles; fluxes are measured × $10^{10}$ mol/year.

**Table 1.** Flux equations of the mass balance model. $F_{ij}$ stands for the elemental flux from reservoir *i* to reservoir *j*; $M_k$ is the mass of reservoir *k*. See text and (10) for justification of the flux equations.

| Carbon | | Phosphorus | | Iron | |
|---|---|---|---|---|---|
| $F_{13} = (C/P)_{Redfield}F_{54}$ | (1) | $F_{54} = k_{54}v_{mix}M_5$ | (5) | $F_{1113} = xF_{1011}$ | (12) |
| $F_{31} = F_{13} - F_{36}$ | (2) | $F_{45} = F_{54} - F_{47}$ | (6) | $F_{1112} = (1-x)F_{1011}$ | (13) |
| $F_{36} = k_{36}F_{13}^{2.5}$ | (3) | $F_{47} = \frac{F_{36}}{(C/P)_{burial}}$ | (7) | $F_{1210} = k_{uplift}M_{12}$ | (14) |
| $F_{61} = k_{uplift}M_6$ | (4) | $F_{58} = k_{58}F_{45}^{2.5}$ | (8) | $F_{1310} = k_{uplift}M_{13}$ | (15) |
| | | $F_{59} = k_{59}F_{1112}$ | (9) | $F_{1011} = k_{1011}M_{10}$ | (16) |
| | | $F_{72,82,92} = k_{uplift}M_{7,8,9}$ | (10) | | |
| | | $F_{25} = k_{25}M_2$ | (11) | | |
| Oxygen | | $\frac{dM_{14}}{dt} = F_{13} - \left(F_{31} - \frac{7.5}{2}F_{1113}\right) - \frac{7.5}{2}F_{1310} - F_{61}$ | (17) | | |
| $DOA = 1 - k_{OA}\left(\frac{v_{mix}M_{14}}{F_{13}}\right)$ | (18) | $\left(\frac{C}{P}\right)_{burial} = \frac{(C/P)_{oxic}(C/P)_{anoxic}}{(1-DOA)(C/P)_{anoxic} + DOA(C/P)_{oxic}}$ | (20) | | |
| $x = 0.44 + 0.56(DOA)$ | (19) | | | | |

and DOA are globally weighted parameters of the world ocean (*10*).

A basic assumption of the model is that the flux of reactive dissolved phosphorus to the photic zone drives oceanic productivity. Mathematically, this means that the rate of net photosynthetic phosphorus fixation is proportional to the product of $v_{\mathrm{mix}}$ and the concentration (mass) of available reactive phosphorus (Eq. 5, Table 1). Net production of organic carbon is obtained from the Redfield C:P ratio of new marine production, which for our purposes is kept constant (Eq. 1, Table 1). The carbon and phosphorus cycles are further linked by the C:P ratio of organic matter that is being buried in marine sediments (Eq. 7, Table 1). On the basis of the observational evidence mentioned earlier, this ratio is postulated to be a function of the degree of anoxicity of oceanic waters (Eq. 20, Table 1). The end-member C:P values of organic matter buried in a completely oxic and a completely anoxic ocean, respectively, were estimated from our sediment data (*9, 13*). DOA itself depends on the relative magnitudes of oxygen demand and supply in the water column (Eq. 18, Table 1). Oxygen consumption below the photic zone is assumed to be directly proportional to the net primary production of carbon exported from the photic zone, whereas ventilation is a function of the rate of vertical mixing and the dissolved oxygen concentration of the surface waters. The latter is assumed to be proportional to the concentration (mass) of atmospheric $O_2$.

The distribution of reactive iron burial between ferric (hydr)oxides and ferrous iron sulfide is a function of DOA (Eqs. 12, 13, and 19, Table 1). In a completely anoxic ocean (DOA = 1), all reactive iron burial is in the form of sulfide-bound Fe(II). However, iron sulfide burial does not vanish when the ocean is completely oxic (DOA = 0), because sulfate reduction remains a major early diagenetic pathway of carbon oxidation in organic-rich sediments deposited below oxygenated waters (*14*). Marine sedimentary burial of reactive phosphate sorbed to iron (hydr)oxides is obtained directly from the burial flux of reactive Fe(III) (Eq. 9, Table 1). The rates of supply of reactive phosphorus and iron to the oceans, primarily from weathering, are assumed to be linear functions of the crustal reservoir sizes (Eqs. 11 and 16, Table 1). The $O_2$ fluxes in and out of the atmosphere are calculated from the overall reaction stoichiometries for net photosynthesis, aerobic respiration, and anaerobic respiration, plus oxidative weathering of organic carbon and pyrite that are generally used by modelers of biogeochemical redox cycles (*4, 5*). The flux equations in Table 1 fully couple the dynamics of the four elemental cycles.

We derived values for the coefficients in the flux equations from the preanthropogenic steady-state biogeochemical cycles (Table 2). For each of the 14 reservoirs in the model (Fig. 1), we calculated the rate of change of the reservoir mass by summing input fluxes and subtracting output fluxes. This produced a set of coupled ordinary differential equations that we integrated numerically and solved for the time-dependent reservoir masses.

In order to investigate the coupled dynamics of the biogeochemical cycles, we carried out a perturbation analysis by imposing a periodically varying $v_{\mathrm{mix}}$ on the system and then characterizing the responses of the various reservoir sizes and material fluxes by their amplitudes and their phase shifts relative to the forcing function. The choice of $v_{\mathrm{mix}}$ as the forcing variable stems from previous work, which has shown that the redox state of the oceans and their biological productivity are strongly dependent on the intensity of global-scale vertical circulation (*10, 15*). By varying the period length of the forcing function, we determined the responses over a range of time scales.

The results of the analysis indicate that fluctuations in marine net primary production, even fairly large ones, have little effect on atmospheric $P_{O_2}$ on time scales shorter than 1 million years (My). This is not unexpected, as the residence time of $O_2$ in the atmosphere is on the order of several million years (*2*) (see also Fig. 1). In other words, only changes in net primary production or, more appropriately, in organic carbon and pyrite burial that persist for more than several million years can potentially modify the $P_{O_2}$ of the atmosphere. Thus, geologic time as used here will be understood to refer to time spans of 1 My or more.

For time scales exceeding 10 My, the degree of anoxicity, marine productivity, and atmospheric $P_{O_2}$ are all approximately 180° out of phase with the rate of ocean mixing. This implies that long-term ocean stagnation should promote net primary production in the oceans and increase the mass of $O_2$ in the atmosphere. The buildup of $P_{O_2}$ with increasing ocean anoxia and, hence, the higher solubility of oxygen in ocean surface waters create a negative feedback that opposes a runaway spreading of water column anoxia during sustained periods of slow overturn. The feedback also prevents the oceans from becoming locked into a permanently anoxic state. The calculations suggest that the world's ocean is unlikely to maintain global-scale bottom water anoxia for periods of time much longer than $10^8$ years, unless thermohaline circulation completely ceases. It is worth emphasizing that in the perturbation analysis, the supply of reactive phosphorus from continental weathering was kept

**Table 2.** Numerical values of model parameters. The kinetic parameters are derived from the reservoir sizes and mass fluxes in Fig. 1.

| Organic matter | Kinetic parameters |
|---|---|
| $(C/P)_{\mathrm{Redfield}} = 106$ | $k_{25} = 2.57 \times 10^{-9}$ year$^{-1}$ |
| $(C/P)_{\mathrm{oxic}} = 200$ | $k_{36} = 1.20 \times 10^{-26}$ (mol/year)$^{-1.5}$ |
| $(C/P)_{\mathrm{anoxic}} = 4000$ | $k_{54} = 3.93 \times 10^{-3}$ m$^{-1}$ |
| | $k_{58} = 5.56 \times 10^{-24}$ (mol/year)$^{-1.5}$ |
| | $k_{59} = 1.71 \times 10^{-2}$ |
| | $k_{1011} = 6.08 \times 10^{-10}$ year$^{-1}$ |
| | $k_{\mathrm{uplift}} = 2.88 \times 10^{-9}$ year$^{-1}$ |
| | $k_{\mathrm{OA}} = 1.73 \times 10^{-5}$ m$^{-1}$ |

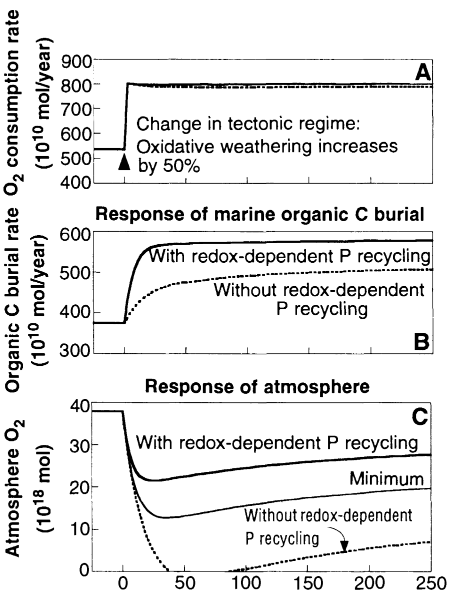

**Fig. 2.** Response to an instantaneous rise of $k_{\mathrm{uplift}}$ by 50%. (**A**) The switch in tectonic forcing causes a step increase in the rate of removal of oxygen from the atmosphere by oxidative weathering. Whether the burial of organic phosphorus in the oceans is a function of water column oxygenation (solid line) or not (broken line) makes little difference to the oxygen removal rate. Calculations without redox dependence of organic phosphorus burial were performed with the use of the following end-member C:P ratios (Eq. 20, Table 1): $(C/P)_{\mathrm{oxic}} = (C/P)_{\mathrm{anoxic}} = 250$ (atomic). Calculations with redox fractionation used $(C/P)_{\mathrm{oxic}} = 200$ and $(C/P)_{\mathrm{anoxic}} = 4000$ (Table 2). (**B**) The onset of uplift is accompanied by a decrease in ocean ventilation. When the effect of water column oxygenation on the oceanic recycling of phosphorus is taken into account, substantially higher levels of marine net primary production and organic carbon burial are obtained. (**C**) Because organic carbon burial represents the main oceanic source of atmospheric $O_2$ on geologic time scales, the more efficient recycling of phosphorus stabilizes atmospheric $P_{O_2}$ by offsetting the increased terrestrial $O_2$ demand. The stabilizing effect is observed even with a minimum estimate of the redox fractionation of organic phosphorus and carbon burial, that is, when $(C/P)_{\mathrm{anoxic}} = 500$ (*13*).

constant, that is, the changes in marine biological productivity and atmospheric $P_{O_2}$ were due only to readjustments of the recycling efficiency of phosphorus in the ocean's water column.

The inverse relation between oceanic water column oxygenation and surface primary production also provides a negative feedback that may help stabilize atmospheric oxygen levels over geologic time. Consider a rise in atmospheric oxygen consumption by oxidative weathering on the continents. Such a situation would arise, for instance, from the rapid exposure to the atmosphere of large amounts of relatively young sediments during an orogenic event, say the uplift of the Himalayas. In itself, the higher rate of oxidative weathering would cause a drop in $P_{O_2}$ and reduce the uptake of oxygen by the oceans. The accompanying decrease in retention of reactive phosphorus by the sediments would stimulate surface water productivity, and the increased net return of photosynthetic $O_2$ to the atmosphere would then counteract the initial decline in atmospheric $P_{O_2}$. The coupled mass-balance model presented here was used for a performance assessment of this feedback mechanism.

We simulated the response of today's atmosphere to a change in the intensity of oxidative weathering by computing the effects of an instantaneous increase of the rate coefficient of uplift ($k_{\mathrm{uplift}}$ in Eqs. 4, 10, 14, and 15, Table 1) by a factor of 1.5 (Fig. 2). In the model, the terrestrial oxygen uptake immediately registers the enhanced exposure rates of reduced carbon and iron (Fig. 2A). We first considered a scenario in which marine phosphorus burial with organic matter is independent of water column oxygenation; that is, the C:P ratio of organic matter being incorporated in the sedimentary column was assigned a constant value, equal to the average estimated for today's ocean. In this case, all oxygen would be completely removed from the atmosphere within 36 My, all other conditions being unchanged (Fig. 2C).

Atmospheric $P_{O_2}$ crashes because the system reacts too slowly to the increased $O_2$ demand caused by oxidative weathering of organic carbon and pyrite on the continents. More reactive phosphorus is being mobilized by weathering on land, but its delayed delivery to the oceans (Fig. 2B) gives the sustained high levels of terrestrial $O_2$ consumption enough time to deplete the atmosphere (*16*). Although the step function used for the rate coefficient of uplift is not intended as a realistic representation of tectonic forcing of biogeochemical cycling, the simulation does illustrate the dramatic impact on atmospheric $P_{O_2}$ that imbalances in the rates of production and consumption of $O_2$ would have if they persist for periods of time in excess of a few million years (*2*).

In the second scenario, the burial efficiency of organically bound phosphorus is assumed to be a function of the oxygenation of oceanic bottom waters, as shown by our data from modern and ancient marine sediments. The proposed redox fractionation between marine sedimentary burial of organic carbon and organic phosphorus effectively buffers the increased consumption of oxygen on the continents. This is the case even when a conservative estimate of the carbon-phosphorus fractionation is used (Fig. 2C). The oxygen catastrophe is averted because the initial decline in atmospheric $P_{O_2}$ causes the oceans to switch to a more efficient recycling of nutrient phosphorus, thereby enhancing net photosynthetic production of $O_2$ and limiting the drawdown of $O_2$ from the atmosphere (*17*). The feedback mechanism also works in the opposite direction by dampening the effects of decreased oxygen consumption by weathering. On geologic time scales, the fast responses of ocean oxygenation, water column recycling of phosphorus, and net primary production cause near instantaneous readjustments in the sedimentary burial of organic carbon plus iron sulfide to changes in the oxygen content of the atmosphere (Fig. 2B).

In conclusion, observational data on benthic phosphorus regeneration in marine depositional environments, combined with mass-balance calculations, support a determining role for oceanic phosphorus cycling in the long-term stabilization of redox conditions of the atmosphere-ocean system. The phosphorus-mediated coupling of ocean productivity and atmospheric oxygen provides effective safeguards against catastrophic depletion or buildup of atmospheric $O_2$ and against the irreversible eutrophication of the oceans. Consequently, the redox-dependent burial of phosphorus in marine sediments may have been instrumental in creating the stable environmental conditions that were necessary for the radiation of higher plants and animals during the Phanerozoic.

## REFERENCES AND NOTES

1. L. V. Berkner and L. C. Marshall, *J. Atmos. Sci.* **22**, 225 (1965); A. Watson, J. E. Lovelock, L. Margulis, *Biosystems* **10**, 293 (1978); T. P. Jones and W. G. Chaloner, *Palaeogeogr. Palaeoclimatol. Palaeoecol.* **77**, 39 (1991); J. M. Robinson, *ibid.*, p. 51.
2. H. D. Holland, *The Chemical Evolution of the Atmosphere and Oceans* (Princeton Univ. Press, Princeton, NJ, 1984).
3. A. C. Lasaga, R. A. Berner, R. M. Garrels, in *The Carbon Cycle and Atmospheric $CO_2$: Natural Variations Archean to Present*, E. T. Sundquist and W. S. Broecker, Eds. (American Geophysical Union, Washington, DC, 1985), pp. 397–411.
4. R. A. Berner, *Palaeogeogr. Palaeoclimatol. Palaeoecol.* **75**, 97 (1989).
5. L. R. Kump and R. M. Garrels, *Am. J. Sci.* **286**, 337 (1986); R. A. Berner, *ibid.* **287**, 177 (1987); L. R. Kump, *Nature* **335**, 152 (1988); R. A. Berner and D. E. Canfield, *Am. J. Sci.* **289**, 333 (1989); L. R. Kump, in *Interactions of C, N, P and S Biogeochemical Cycles and Global Change*, R. Wollast, F. T. Mackenzie, L. Chou, Eds. (Springer-Verlag, Berlin, 1993), pp. 475–490.
6. H. D. Holland, *Nature* **347**, 17 (1990).
7. A. C. Redfield, *Am. Sci.* **46**, 205 (1958); H. D. Holland, *The Chemistry of the Atmosphere and the Oceans* (Wiley-Interscience, New York, 1978); W. S. Broecker, *Geochim. Cosmochim. Acta* **46**, 1689 (1982). On time scales of days to decades, local nutrient limitation may be complex and temporally variable, with more than one limiting factor being involved in setting the level of net primary production. The productivity of a global ecosystem integrated over a long time, however, will approach the single limiting nutrient end-member situation. Phosphorus is the most likely limiting nutrient for global ocean productivity on geologic time scales, because any long-term nitrogen deficiency can be made up by increased nitrogen fixation from the atmosphere.
8. G. M. Filippelli and M. L. Delaney, *Paleoceanography* **9**, 643 (1994); K. B. Föllmi, *Geology* **23**, 859 (1995).
9. E. D. Ingall, R. M. Bustin, P. Van Cappellen, *Geochim. Cosmochim. Acta* **57**, 303 (1993); E. Ingall and R. Jahnke, *ibid.* **58**, 2571 (1994); *Mar. Geol.*, in press. In modern depositional environments, benthic chamber flux experiments combined with measured burial rates provide direct evidence for decreased burial efficiencies of phosphorus when bottom waters are low in oxygen. This is consistent with data from ancient sediments, in which the organic matter preserved in finely laminated shales is found to be strongly depleted in phosphorus relative to that in bioturbated shales of the same sequences.
10. P. Van Cappellen and E. D. Ingall, *Paleoceanography* **9**, 677 (1994). Global-scale anoxia-dysoxia results in a more efficient recycling of reactive phosphorus in the oceans, and hence higher rates of primary production and organic carbon burial. The positive feedback between oxygen depletion of bottom waters and benthic phosphorus regeneration may be one of the mechanisms driving ocean anoxic events.
11. R. Raiswell, unpublished data. The reactive fraction of sedimentary iron is on the order of 20 to 25% in most modern marine depositional environments. Values of up to 70 to 80% are found in certain euxinic environments. On a global basis, sulfide-bound Fe(II) represents 56% of the reactive iron in marine sediments (range: 12 to 85%).
12. W. S. Broecker and T. H. Peng, *Tracers in the Sea* (Eldigio Press, Palisades, NY, 1982).
13. Data from both modern and ancient marine sediments indicate that the atomic C:P ratios of organic matter buried under completely anoxic bottom waters are at least on the order of 500 to 1000 (*9*). Here we use a value of 4000, which is the average value for organic matter in laminated Phanerozoic black shales that have not undergone significant late diagenetic alteration. We have also shown that ocean productivity is not very sensitive to variations in the anoxic end-member C:P ratio, once the latter exceeds 1000 (*10*).
14. D. E. Canfield, *Deep Sea Res.* **36**, 121 (1989); T. K. Tromp, P. Van Cappellen, R. M. Key, *Geochim. Cosmochim. Acta* **59**, 1259 (1995).
15. J. L. Sarmiento, T. D. Herbert, J. R. Toggweiler, *Global Biogeochem. Cycles* **2**, 115 (1988); T. D. Herbert and J. L. Sarmiento, *Geology* **19**, 702 (1991).
16. In order to create an imbalance in oxygen consumption and production at the onset of uplift, the model deliberately allows for some degree of decoupling of oxidative weathering and riverine supply of reactive phosphorus to the oceans. Exposure of reduced carbon and iron on land results in the immediate removal of $O_2$ from the atmosphere. For phosphorus, however, there is a lag between terrestrial exposure and delivery to the oceans. Such a lag is not unreasonable, especially in view of the poor correlation between marine phosphorus burial and crustal uplift reported for the past 32 My (*8*).
17. The burial rates of both organic phosphorus and Fe(III)-bound phosphorus increase when the oceanic water masses become more oxygenated and vice versa. Thus, the two sedimentary P sinks contribute to the stabilizing effect on atmospheric $O_2$ proposed here. Quantitatively, however, burial of organic P is the more important process.
18. Supported by the donors of the Petroleum Research Fund, administered by the American Chemical Society (28069-AC2 to P.V.C.), and by NSF (OCE94-15563 to E.I.). We thank R. Raiswell for sharing his unpublished results.

19 October 1995; accepted 20 November 1995